X-Ray Fluorescence Investigation of the Shroud of Turin

R.A. Morris, L.A. Schwalbe and J.R. London
Shroud of Turin Research Project, Inc., PO Box 7, Amston, Connecticut 06231, USA

We present results of X-ray fluorescence measurements on the Shroud of Turin. Quantitative estimates are given for the observed trace quantities of calcium, iron and strontium, and detection limits are established for other elements of potential interest. The calcium and strontium appear as uniform background distributions. Iron traces are observed in all of the data spectra but their local concentrations vary. Comparisons between image and off-image areas reveal no differences, within the precision limits of the data, that would indicate the presence of pigments or dyes containing high-C elements. In 'blood' stain regions the measurements show significantly higher concentrations of iron. However, the data do not allow a unique identification of the stain's origin. Quantitative comparisons are made between the shroud results and similar measurements on whole blood and Fe_2O_3 stains.

INTRODUCTION

The Shroud of Turin is a linen cloth that dates from at least the middle of the 14th century.[1] It is traditionally considered to be the burial cloth of Jesus Christ in which the body was wrapped after it was taken from the cross. Two halves of the 1.1 m × 4.3 m cloth are shown in Figs 1 and 2. The most obvious visible features on the shroud are the two series of scorch marks, burned holes and patches that run its length. The damage resulted from a fire in 1532 and the patches were subsequently sewn over the more serious holes. The most interesting feature of the cloth, however, is the head-to-head frontal and dorsal image of a nude male on the fabric surface. In the regions of the head, wrist, side and feet of the image there are carmine-colored 'blood' stains that have permeated the cloth.

This paper is a description of the techniques used and the results obtained from X-ray fluorescence measurements on the shroud. The experiment is only one in a series performed under the auspices of the Shroud of Turin Research Project Incorporated. The tests were performed in one wing of the Savoy Palace in Turin during the week of 8 October 1978 and were intended to produce a body of scientific data that might be used to determine the nature of the image and stains. The other work included fluorescence and reflectivity measurements in the infrared, visible and ultraviolet portions of the spectrum as well as low-energy radiography.

The primary goal of the X-ray fluorescence experiment was to provide estimates of elemental variations among the following areas of the cloth:

(1) 'blood' stains;
(2) image areas ('non-blood');
(3) 'pristine' cloth (background);
(4) scorch areas; and
(5) patches.

The available equipment allowed detection of elements with atomic numbers greater than 16. With this information the relative concentrations of observed elements can be correlated with visible features or historical events and be applied to test various image forming hypotheses.

PROCEDURE

During this experiment the shroud with its attached backing cloth was mounted vertically on a special frame that permitted removal of rear support panels from behind the areas inspected. The 50 pkV Balteau tungsten-target X-ray tube used for the low-energy radiography study[2] was adopted as the primary excitation source. The geometry of the source—detector system is illustrated schematically in Fig. 3.

The tube was operated at 50 pkV and 20 mA, its maximum rated power level, and was oriented to illuminate a thick tin target plate which acted as a secondary emitter. The lead tube housing was designed to shield the environment from X-radiation while allowing a fairly well-defined beam of Sn K-series radiation to emerge through the exit port. A 12 μm thick silver foil located over the exit port acted as a 'notch' filter that effectively removed the Sn Kβ lines and scattered high-energy continuum radiation as well as lower energy components with varying degrees of efficiency. The source—collimator system thus produced a nearly monochromatic beam of 25.5 keV Sn Kα X-rays incident to the cloth surface at an angle of about 45°.

We used a Kevex Model 3040 Si(Li) detector with a nominal resolution of 160 eV FWHM. A lead shield with a 4 mm diameter collimation hole fitted over the detector. The geometry of the detector system, illustrated in Fig. 3, defined the 1.3 cm^2 sample area on the cloth. The X-ray tube, detector and lead shields were mounted on a prealigned plate that was supported by a heavy duty tripod. For a series of spectra, we positioned and aligned the system toward a well-defined spot on the shroud and then simply raised or lowered it as a unit to collect data along a scan line.
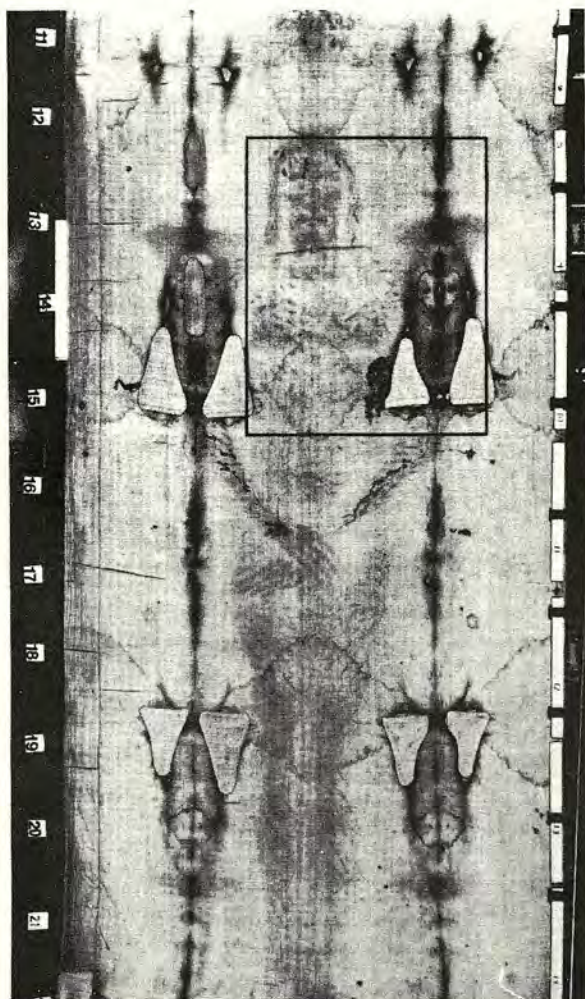
Figure 1. Photograph of shroud area containing full frontal image. The outlined region is shown in greater detail in Fig. 5.
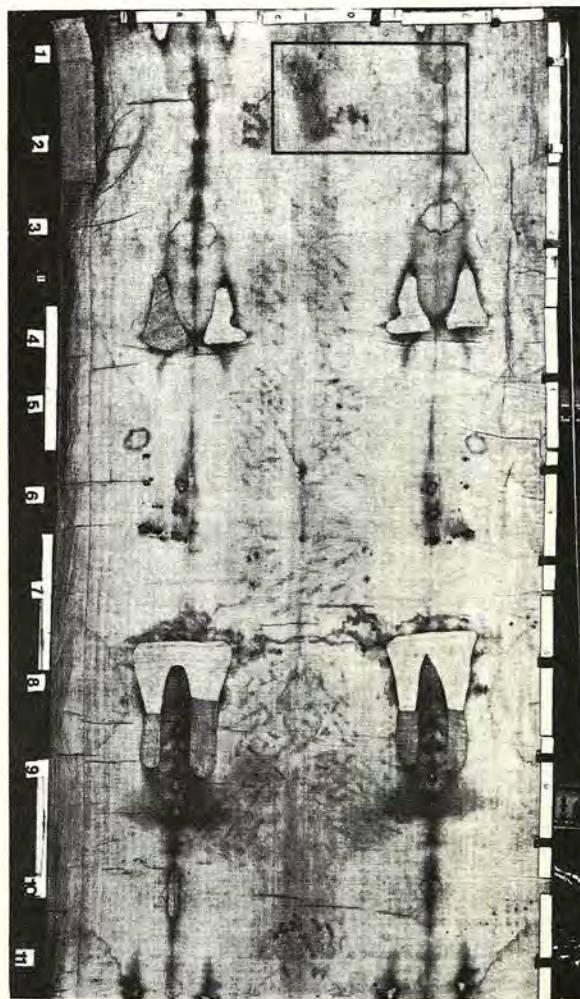

Figure 2. Photograph of shroud area containing full dorsal image oriented with the head at the bottom of the figure. The outlined region is shown in greater detail in Fig. 4.

Detector pulses were processed in a linear amplifier with a zero to 5 V output and stored in 512 channels of a Canberra Model 3100 pulse height analyzer. After accumulating each spectrum, we recorded the data on a Canberra Model 5411 digital tape cassette for subsequent analysis.

Energy calibration spectra were taken using titanium and copper foils as standards. The measured positions of the K-fluorescence lines in these spectra and their tabulated energy values determined a linear calibration curve. We collected calibration spectra before, during and after the data runs. The only change in calibration over the entire 30 hour data collection period was an offset of 0.020 keV in the intercept.

We collected a total of 37 spectra; these included room and instrumentation background, calibration and shroud data. The latter were chosen to cover a wide range of image intensities as well as cloth background and 'blood' stains. Two scans of data, one near the dorsal foot image (1–7) and one across the face (9–18), are mapped in Figs 4 and 5 respectively. In addition to these, we collected individual spectra over an anomalous dark spot on the foot (8), a pristine cloth area (19), a scorch (20), a sewn patch (21),
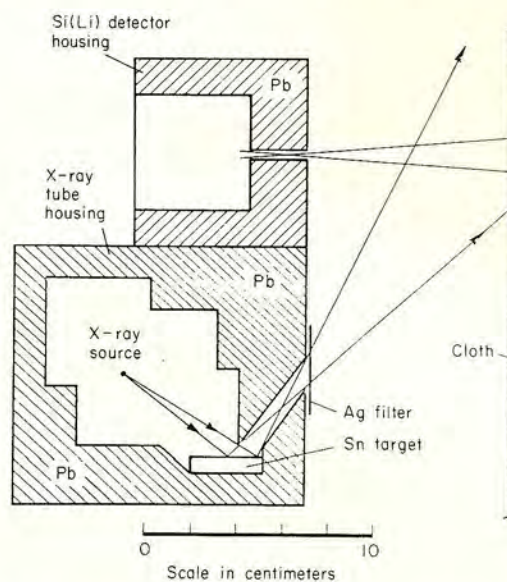

Figure 3. Schematic diagram of shroud, detector and tube housing configuration.
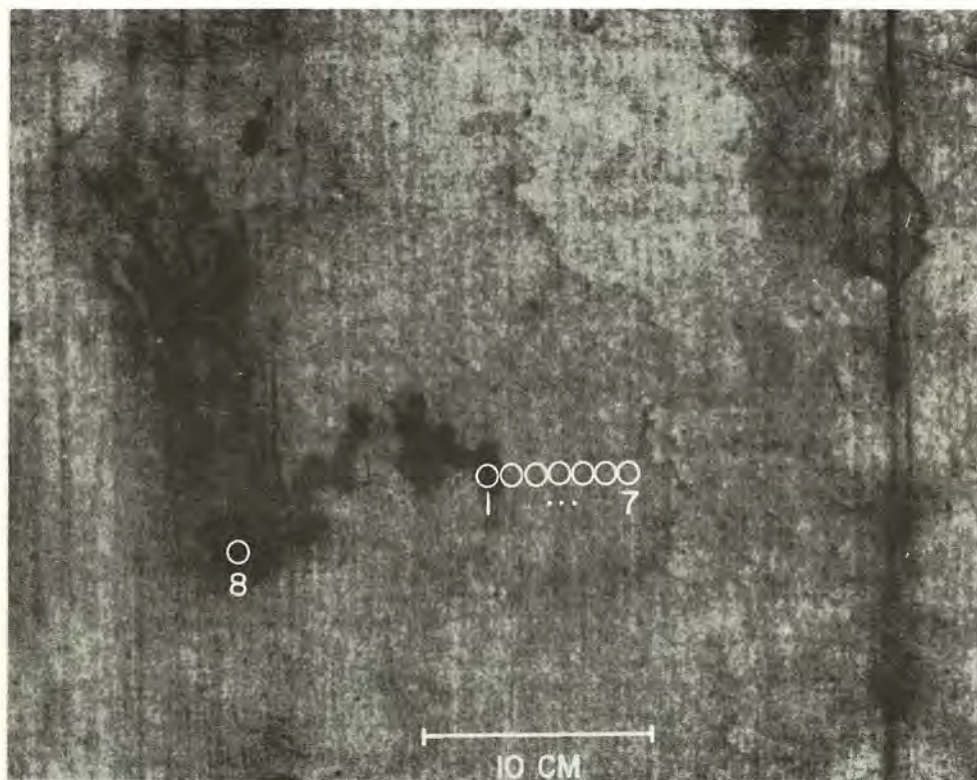
Figure 4. Photograph of the dorsal-foot image area on the shroud. Measurement locations are designated by their corresponding data spectrum number.

one eye (22) and the 'blood' stain at the side (23). The low-energy radiographs[2] showed no obvious high-Z inclusions in any of these areas.

We had hoped to inspect as many points on the cloth as possible in the limited time available for the study. It was therefore necessary to compromise the individual counting times and the data precision considerably. Counting periods of 2000 s were taken and will be assumed unless noted otherwise.

DATA ANALYSIS AND DISCUSSION

Cloth density

A typical spectrum is shown full-scale in Fig. 6. Although this particular one was taken over the 'nose' on the image, on this scale all of the spectra appear nearly identical. The most obvious common feature of the data is the broad but strong Sn Kα Compton peak[3] located in the range 23.0–23.5 keV. If the incident X-ray flux is known, the intensity of this peak provides a measure of the amount of material being examined.

After the data collection was completed in Turin, a reassembly of the experimental setup was made at Los Alamos with similar apparatus. This included the same tin target and lead tube and detector housings as used in Turin but with our own General Electric XRD-5 X-ray generator and Machlett AEG-50 tungsten target tube operated at the same pkV and mA noted above.

With this system we calibrated Sn Kα Compton scatter intensity against areal density of cellulose to about 70 mg cm^{-2} using various numbers of single thickness Whatman 42 filter paper sheets (10.4 mg cm^{-2} nominal densities). A plot of these calibration data showed a slight curvature above about 40 mg cm^{-2} which indicates the small but non-negligible cellulose attenuation of these energy X-rays. In the range below 60 mg cm^{-2}, Compton scatter intensities from test linen samples agreed with those from filter paper of equivalent areal densities.

One of the background runs in Turin was a 2000 s air scatter measurement. By collecting the equivalent spectrum in Los Alamos and correcting for atmospheric pressure differences,[4] we were able to calculate a factor from the ratio of the two Sn Compton peak counts which correlated the excitation flux intensities of the Balteau and GE machines. In Table 1 we have listed the Compton scatter intensities of the individual shroud data spectra expressed in terms of areal cellulose density from our calibration curve. These densities refer to a double thickness of cloth – the holland cloth backing could not be removed from the shroud itself.

The accuracy of these numbers is limited primarily by the counting statistics of the Turin air scatter data. We estimate an uncertainty of about 10% in the excitation flux correlation factor. Since this error only pertains to a common scale factor for the numbers appearing in Table 1, the large individual variations might be attributed to corresponding cloth inhomogeneities. Those of the foot scan, for instance, are uniformly greater in density which may
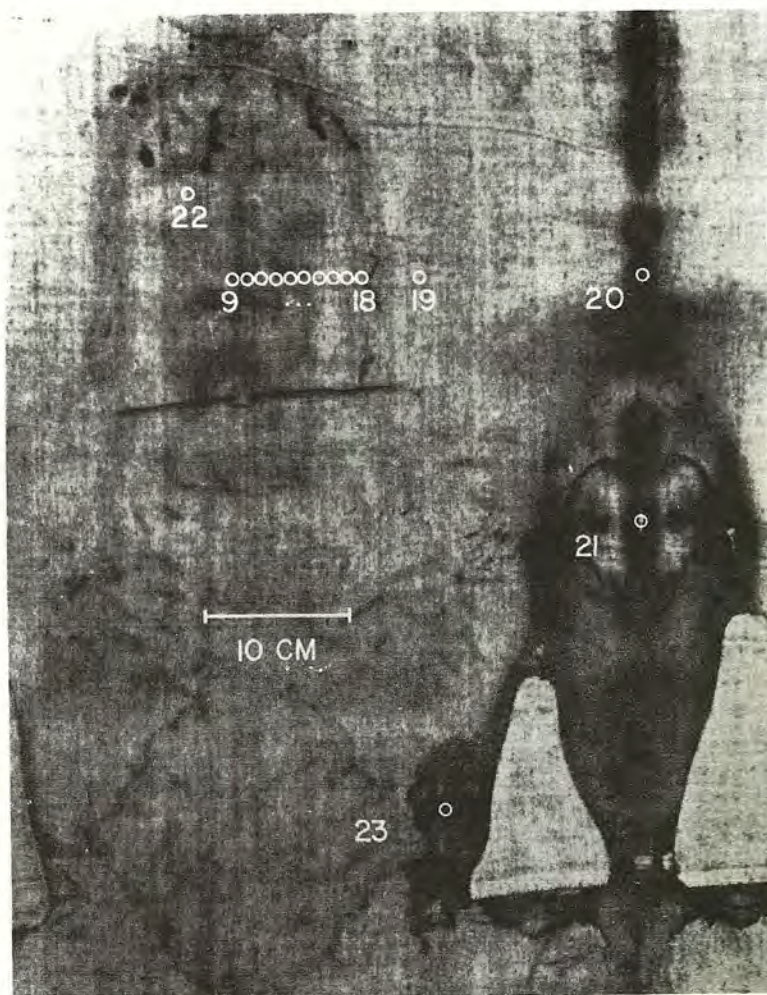
Figure 5. Photograph of the frontal-face and upper-torso image area on the shroud. Measurement locations are designated by their corresponding data spectrum number.

indicate a heavier warp thread used in that region. We note, however, that the results can be influenced significantly by instabilities in the X-ray tube output intensity as well as by misalignments of the apparatus. The alignment problem can
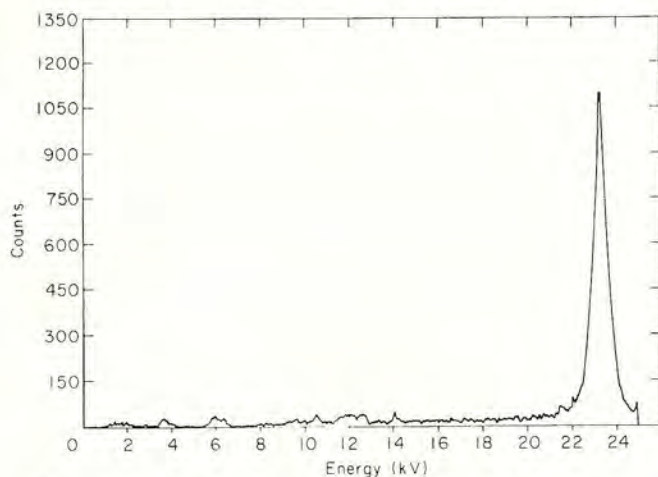

Figure 6. Full-scale representation of data spectrum 9 taken over the 'nose' area on the face image.

by itself introduce errors as large as 10%. In view of these uncertainties, the areal densities in the table do not appear unreasonable when compared with the average value of 24.5 mg cm^{-2} estimated by Timossi[5] for the shroud alone, particularly since a corresponding value for the backing cloth is not available.

Qualitative analysis

The remaining discussion pertains mainly to the spectral characteristics in the energy range 1–20 keV. A signal was seen at about 0.5 keV in all spectra at the foot (1–8) and only these. However, with the apparatus described, we do not expect meaningful data at these low energies. We believe the origin of the artifact is probably electronic and will ignore it, at least tentatively, in the remaining discussion.

An electronic noise peak at 6.0 keV was evident in all of the spectra including several taken with the X-ray tube off and the detector directed away from the shroud. Although it interfered seriously with the Fe Kα at 6.4 keV, we were able to estimate the intensity of the electronic artifact from several such background measurements. The iron trace quantities, discussed below, were determined only after this

Table 1. Linen areal densities and trace element weight fractions for the individual data spectra

Spectrum number	Density (mg cm⁻²)	Calcium (µg cm⁻²)	Iron (µg cm⁻²)	Strontium (µg cm⁻²)
1[a]	39.9 ± 0.7	213 ± 24	58.0 ± 2.9	2.7 ± 0.8
2	39.7 ± 1.0	216 ± 24	51.8 ± 2.8	2.2 ± 0.8
3	41.5 ± 1.0	250 ± 25	34.1 ± 2.5	2.8 ± 0.8
4	42.1 ± 1.1	209 ± 24	33.1 ± 2.5	3.3 ± 0.8
5	40.4 ± 1.1	253 ± 25	35.6 ± 2.6	2.9 ± 0.8
6	37.7 ± 1.0	197 ± 24	29.2 ± 2.5	2.7 ± 0.8
7	38.5 ± 1.0	191 ± 24	24.7 ± 2.4	2.9 ± 0.8
8[b]	34.5 ± 1.0	237 ± 44	39.1 ± 4.2	2.3 ± 1.5
9	33.0 ± 0.9	188 ± 24	16.8 ± 2.3	1.9 ± 0.8
10	34.5 ± 0.9	225 ± 24	17.5 ± 2.3	1.9 ± 0.8
11	36.2 ± 1.0	206 ± 24	12.5 ± 2.2	2.3 ± 0.8
12	35.3 ± 1.0	197 ± 24	13.0 ± 2.2	2.8 ± 0.8
13	33.8 ± 1.0	200 ± 24	10.6 ± 2.2	1.8 ± 0.8
14	33.3 ± 1.0	175 ± 23	10.1 ± 2.2	2.0 ± 0.8
15	34.4 ± 0.9	194 ± 24	8.3 ± 2.1	2.1 ± 0.8
16	32.7 ± 1.0	191 ± 24	9.6 ± 2.1	2.2 ± 0.8
17	32.0 ± 1.0	206 ± 24	11.8 ± 2.2	2.0 ± 0.8
18[a]	32.0 ± 1.0	181 ± 23	16.5 ± 2.3	1.7 ± 0.8
19	29.2 ± 0.8	116 ± 22	6.8 ± 2.1	0.6 ± 0.8
20	31.7 ± 1.0	184 ± 23	13.5 ± 2.2	1.0 ± 0.8
21	34.0 ± 1.0	160 ± 23	13.8 ± 2.2	1.2 ± 0.8
22	35.4 ± 0.9	244 ± 25	10.8 ± 2.2	2.7 ± 0.8
23[a]	32.0 ± 0.9	200 ± 24	50.0 ± 2.8	2.1 ± 0.8

[a] 'Blood' stain measurement.
[b] 1000 s counting period.

averaged noise intensity was subtracted from that of the composite peak.

Besides these electronic noise signals, the data contained more interesting features. Several are evident in the spectra illustrated in Fig. 7. Figure 7(a) is an expanded-scale version of spectrum 9 that appeared earlier in Fig. 6. It is included here as a typical 'non-blood' measurement. We found that all spectra from the 'non-blood' areas were qualitatively quite similar to one another and that they could generally be distinguished from those taken at the 'blood' stains.

To illustrate the major difference between the 'blood' and 'non-blood' sets, in Fig. 7(b) we have included spectrum 23 from the 'blood' wound on the side. Besides the differing random noise characteristics of Fig. 7(a) and (b) (these examples well illustrate the poor signal-to-noise ratio typical of all the data), the obvious distinguishing features of the 'blood' spectrum are the pronounced peaks at 6.4 keV and 7.0 keV. These signals correspond to the Kα and Kβ peaks of iron and indicate a significantly higher concentration of this element than that found in 'non-blood' areas. Quantitative estimates of these traces will be made later in the paper.

A number of features common to these two spectra could be pointed out; however, better representations of the qualitative spectral characteristics are possible from data composites. An average of the face scan spectra (9–19) is shown in Fig. 8(a). The seven spectral features labelled in this plot are common to all of the data spectra.

Below the composite we have included as Fig. 8(b) a spectrum taken from Whatman 42 filter paper. The purpose of this 'control run' was to help qualitatively identify spectral artifacts resulting from primary beam scatter. First, in an independent analysis of the paper, we found no significant quantities of elements which might fluoresce in

the energy range of interest. (The fluorescence lines from the cellulose itself are too low in energy to be detected by our apparatus.) Second, in the results of the follow-up studies, there were no electronic artifacts of the type observed in the Turin data. Therefore, any signals found in the spectrum from the filter paper must have resulted
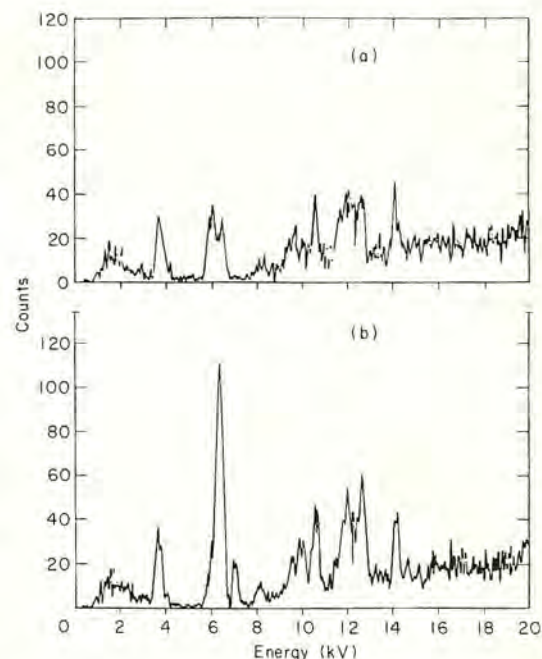

Figure 7. (a) Spectrum 9 shown on an expanded scale. (b) Spectrum 23 taken over the side wound 'blood' stain area.
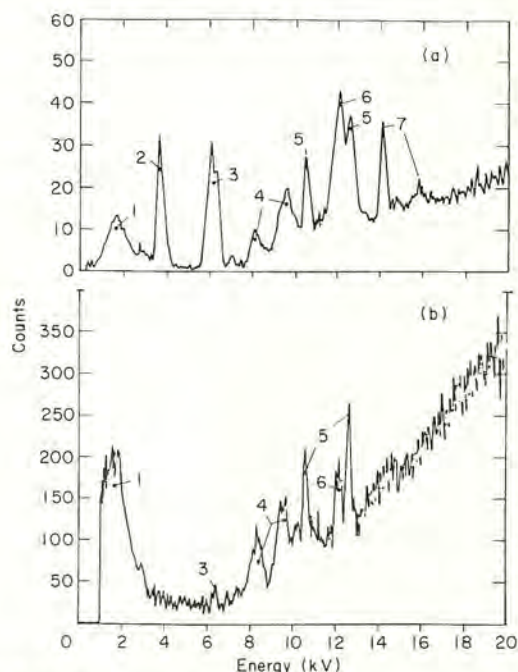
Figure 8. (a) Composite or average of the face-scan measurements. (b) Spectrum taken from five thicknesses of Whatman 42 filter paper. 200 min count.

from scattered radiation. The spectral features common to Fig. 8(a) have been labeled in Fig. 8(b).

The broad feature labeled '1' is scattered low-energy continuum radiation. At 6.4 keV, labeled '3', we see a small Fe Kα signal which is probably coherently scattered fluorescence radiation from a contaminated tin target. The broad peaks centered about 8.2 keV and 9.6 keV, labeled '4', we identify as multiply-scattered tungsten L-lines from the X-ray tube target. The sharper features at 10.5 and 12.6 keV, labeled '5', are lead L-lines that scattered higher energy radiation excites from the detector housing port — they disappear when the detector housing is replaced by an aluminum mask. This secondary fluorescence effect, in particular, greatly reduced the detection sensitivity to traces of lead on the shroud. Finally, the peak labeled '6' at 12.1 keV is contributed at least in part by the Compton scattered Pb Lβ X-rays generated in the exit port of the lead tube housing.

The remaining peaks in Fig. 8(a) are fluorescence signals from trace elements on the shroud. In all of the spectra a slightly skewed peak, labeled '2', at 3.7 keV and two others, labeled '7', at 14.1 keV and 15.8 keV appeared with little variation in intensity. These we recognize as characteristic calcium and strontium K-series X-rays, respectively. The peak labeled '3' is the composite electronic noise signal at 6.0 keV mentioned earlier and the Fe Kα. Our results suggest that these traces are not unique to the original cloth. Spectrum 21, taken over a small patch which was sewn onto the shroud after the 1532 fire, indicated elemental concentrations similar to those present in other areas.

Quantitative analysis

Calibration. To determine weight concentrations, we constructed calibration curves from trace element standards

for calcium, iron, lead and strontium purchased from Columbia Scientific Industries. The standards were nominal 5, 20 and 50 μg cm^{-2} for iron and lead, 50 and 100 μg cm^{-2} for calcium and 20 and 100 μg cm^{-2} for strontium. The excitation flux correlation factor derived for the areal cloth densities calculation was again used. The results for the calcium, iron and strontium traces on the shroud are included in Table 1.

The indicated uncertainties represent one standard deviation for these values and were derived from the counting statistics of the fluorescence signals. For strontium this represents the major accuracy limitation. The calcium and iron numbers are probably each correct within common scale factors to about 20%. The uncertainty in the flux correlation factor, which we estimated to be about 10% in the above discussion, partly accounts for the total error limits. The remainder for calcium results from the long extrapolation from the limited calibration range. That for iron arises from the additional uncertainty in the intensity of the interfering electronic noise signal.

Calcium and strontium. The relatively large proportion of calcium (~ 1 wt %) is most likely underestimated in these results because no account was taken of its distribution within the cloth. X-ray attenuation by hydrocarbons is greatest at lower energies and in these measurements would strongly suppress the calcium peak. We measured an attenuation of approximately 75% for Ca Kα X-rays through 20 mg cm^{-2} cellulose. If the calcium were distributed uniformly through the cloth instead of at the surface, the actual weight concentrations could be twice as large as the numbers quoted. The results for iron would also be affected in a similar but less dramatic way; the same experiment on Fe Kα indicated an attenuation of only 30%.

Both calcium and strontium are relatively common elements. For instance, we might expect considerable quantities of airborne $CaCO_3$ from the rich marble and limestone regions of northern Italy. In igneous rocks strontium occurs as a substitutional element for calcium and potassium in plagioclase and potash feldspars respectively.[6] These minerals are both quite susceptible to weathering and represent major sources of clay in some areas.[7] Although other explanations are possible, the uniform calcium and strontium distributions might be explained simply as dust accumulations.

Iron. Our measurements do reveal a nonuniformity in the background distribution of iron. Figure 9 contains observed iron concentrations plotted against distance for both foot and face scans. The first two measurements at the foot (1 and 2) indicate the higher iron density that is apparently characteristic of the 'blood' regions.[8] The data following these are from the adjacent background containing neither 'blood' nor image. They show significantly higher iron than any of the facial *image* areas investigated.

One of the fundamental questions of the entire study is whether the image had been produced or altered by some form of applied pigments or dyes. A goal of the X-ray fluorescence study was to address this question by revealing any elemental composition differences between image and off-image areas. Generally we have found no significant differences but must establish limits of detectability and sensitivity to make this conclusion meaningful.

To our knowledge, at present only one serious candidate, Fe_2O_3 (jeweler's rouge), has been proposed as an image
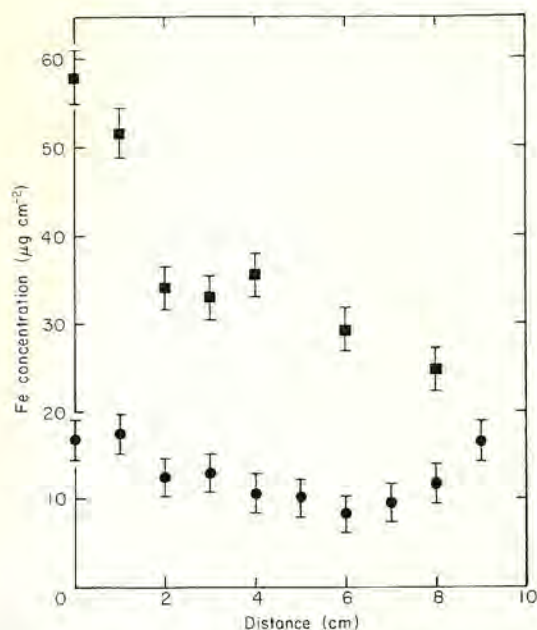
Figure 9. Iron concentrations versus distance along the foot scan (■) (1—7) and along the face scan (●) (9—18).

coloring agent. Even its use is now considered limited at most to the enhancement of some faint pre-existing image.[9] We prepared a series of Fe_2O_3 stains of varying densities in the range below 60 $\mu g\,cm^{-2}$ on filter paper. Microscopically these appeared as uniformly distributed, approximately micrometer-sized particles on the surface fibers of the paper. We then measured reflected densities through several optical filters and plotted the results against iron concentration.

For the neutral density filter the initial slope was 0.01 μg Fe per cm^2. For the shroud measurements we estimate a sensitivity to ± 5 μg per cm^2 changes in iron concentration. The test indicates, therefore, that iron fluorescence signal intensities in the shroud image areas should correlate with reflected density variations larger than 0.05 if the Fe_2O_3 hypothesis were valid. We believe this precision is not sufficient to adequately test the theory and suggest that sensitivity limits of future experiments be greater by at least a factor of 5 than those attained here. Moreover, in view of the sizable background variations, they should also include a greater number of sampled areas.

From the plot of Fig. 9 we find the excess iron concentration in the foot 'blood' region to be about 20 $\mu g\,cm^{-2}$ above background, whereas that for the smaller flow at the side of the face (18) appears to be hardly detectable above the average face-scan value. Excess iron levels for the side wound (23) are difficult to determine because corresponding background levels in the adjacent regions are not available. The data may indicate as much as 30—40 $\mu g\,cm^{-2}$ iron if the face-scan values are taken as reasonable estimates of the background near the side wound.

Although these numbers do not prove that the stains are blood, they are generally consistent with this hypothesis. We measured whole blood iron concentrations to be about 0.5 $\mu g\,mm^{-3}$ and found that roughly 25 mm^3 saturated a 1 cm^2 area of 10 $mg\,cm^{-2}$ Whatman 42 paper. In these

measurements we also observed potassium in addition to iron. The K Kα peak intensity was typically at least an order of magnitude smaller than the Fe Kα. Although no potassium was observed in any of the shroud data, poor signal-to-noise ratios may preclude definite conclusions on this point.

Other elements. In certain archeological studies,[7] relative trace concentrations of strontium, rubidium and zirconium in pot sherds have been used to identify common clay sources. With the Sn Kα excitation radiation used here, detection sensitivities for rubidium, yttrium and zirconium are comparable to that for strontium. Besides strontium, we have detected no signals to suggest the presence of any of these other elements and place upper limits of 0.5 $\mu g\,cm^{-2}$ on their concentrations.

The scattered radiation interferences discussed in connection with Fig. 8(b) limit detection sensitivity for several other potentially interesting elements. The most severe problem is with lead. We place an upper limit of 15 $\mu g\,cm^{-2}$ for lead in our data. Similar limits of 5 $\mu g\,cm^{-2}$ are estimated for copper and arsenic. The broad peak at 12.0 keV in Fig. 8(a) suggests the presence of bromine; however, for the present, we will disregard this possibility since no indication of the Br Kβ is seen at 13.2 keV.

We note, finally, that the use of Sn Kα excitation radiation almost entirely precludes detection of silver, cadmium and tin traces. Their L-series fluorescence signals could be seen only if the elements were present in substantial quantities.

CONCLUSION

We have presented the results of a series of X-ray fluorescence measurements on the Shroud of Turin. There appears to be no evidence of heavy element concentration differences between image (non-blood) and off-image points which would suggest an obvious forgery. The data indicate generally uniform distributions of calcium and strontium over the investigated areas of the cloth. We suggest that these quite possibly represent airborne dust deposits.

Substantially non-uniform concentrations of iron were observed, particularly at the dorsal-foot and side-wound 'blood' stain regions. However, we can say no more than that either blood or some iron-based pigment was used to produce the stains.

In view of the experimental difficulties discussed and despite the conclusions reached thus far, we feel that this work can only represent a preliminary investigation of the problem. A more comprehensive study, one which realizes the full potential of the X-ray fluorescence technique, is clearly called for. On the basis of this work we offer the following points which might be considered in any future X-ray fluorescence investigation.

Either well-characterized continuum or radioisotope sources would be preferable to the experimental arrangement used in the present study. Radioisotope sources are especially convenient and reliable. However, we caution that considerable advanced planning is required for their overseas transport because of rather extensive restrictions. In particular, iron-55 provides far greater sensitivity in the energy range below 5 keV where aluminum, sulfur and

potassium traces might be detected. Cadmium-109 can be used for the energy range from 1 keV to 20 keV. Although background levels are generally greater, the artifacts illustrated in Fig. 8(b) would no longer be present. Finally, with a samarium-145 source the energy range below about 35 keV could be studied for silver, cadmium and tin.

Longer counting times are essential for increased data precision. We suggest periods as long as several hours depending on the particular area studied.

This experiment was performed on the shroud without having the backing cloth first removed. Some ambiguity is therefore inherent in a full interpretation of the results. We feel that this problem is minimized to some extent by our general-survey approach to detect high-Z element differences among 'blood' stain, image and background areas. Nevertheless in any subsequent study, this problem should be avoided before definite conclusions are reached from measured trace element distributions.

REFERENCES

1. We recommend the following readable popular accounts: I. Wilson, *The Shroud of Turin*, Doubleday, Garden City, NY (1978). T. Humber, *The Sacred Shroud*, Pocket Books, New York (1977). For more technical information: Proceedings of the 1977 United States Conference of Research on the Shroud of Turin, Holy Shroud Guild (1977); and Report of Turin Commission on the Holy Shroud, Screenpro Films, 5 Meard St, London WIV 3HQ (1976).
2. W. Mottern, R.A. Morris and J.R. London, to be published.
3. The Compton signal results from an inelastic scattering process between the excitation radiation and the electrons in the cloth. The effect is discussed in somewhat greater detail in E.P. Bertin, *Principles and Practice of X-ray Spectrometric Analysis*, pp. 68–73, Plenum Press, New York (1975).
4. Atmospheric pressure in Los Alamos is nominally 580 torr compared to 745 torr in Turin at the time of the measurements.
5. V. Timossi, *La S. Sindone nella sua constituzione tessile*, Torino (1933).
6. B. Mason, *Principles of Geochemistry*, 3rd edn, pp. 104, 135, Wiley, New York (1966).
7. C. Dipeso, J. Rinaldo and G. Senner, *Casas Grandes: A Fallen Trading Center of the Gran Chichineca*, Vol. 6, Amerind Foundation, Dragoon, Arizona, Northland Press, Flagstaff, Arizona (1974).
8. Although data spectrum 2 is shown as a background point in Fig. 4, its proximity to the stain suggests that a substantial portion of the 'blood' was sampled. Any interpretation of the relatively high iron concentration observed in this particular measurement is subject to some ambiguity.
9. W.C. McCrone, 2nd Workshop on the Shroud of Turin, Los Alamos NM (unpublished).